 https://doi.org/10.3311/PPci.13084

Periodica Polytechnica Civil Engineering, 63(2), pp. 456–464, 2019

Establishment of Coal-rock Constitutive Models for Numerical Simulation of Coal-rock Cutting by Conical Picks

Shuo Qiao[1,3], Jingyi Xia[2], Yimin Xia[1,3*], Zaizheng Liu[4], Jinshu Liu[4], Ailun Wang[1,3]

[1] Institute of Light Alloy, Central South University, Changsha, 410083, China
[2] School of Materials Science and Engineering, Central South University, Changsha, 410083, China
[3] State Key Laboratory of High Performance Complex Manufacturing, Changsha, 410083, China
[4] China Railway Construction Heavy Industry Co., LTD, Changsha, 410100, China
[*] Corresponding author, e-mail: xiaymj@mail.csu.edu.cn

Received: 04 September 2018, Accepted: 29 January 2019, Published online: 04 April 2019

Abstract

One of the key points in numerical simulation of coal-rock cutting by conical picks is to select a proper coal-rock constitutive model. In order to find a reasonable coal-rock constitutive model, a uniaxial compression test was conducted to obtain the constitutive model. The several stages for linear elastic deformation and creep, plastic yielding, hardening, and finally brittle cracking of the constitutive units were studied, and the coal-rock constitutive model was established. As a result, the coal-rock cutting by one conical pick or two conical picks was simulated and the results were compared with coal-rock cutting experiment on a Coal-rock Cutting Machine. According to the simulation and experimental results, it is believed that the numerical simulation can reveal coal-rock crushing process. And the total error rate of coal-rock cutting by one conical pick between the simulation and experiment is 8.5%. The maximum deviation of coal-rock cutting by two conical picks between the simulation and experiment is 9.8%. All simulation values are within a reasonable range. The comparison indicates that the coal-rock constitutive model should better be defined considering the coal-rock crushing process by conical picks.

Keywords

coal-rock constitutive model, conical pick, Weibull Distribution, coal-rock cutting, error analysis

1 Introduction

With the rise of mining mechanized level, the conical pick has been widely used in mining [1–6]. Its disturbance to coal–rock mass directly affects the safety production of coal mines (see Fig. 1). In this case, it is very important to determine the constitutive model of coal-rock to reflect the actual situation in coal mining process by numerical simulation method. At present, many kinds of constitutive models of rock are included in the numerical software. In the selection of constitutive models, it is necessary to select suitable constitutive models for different rock masses, so as to avoid using too simple models which cannot reflect the main characteristics of rock. It is also necessary to avoid using too complex models with many parameters to be determined.

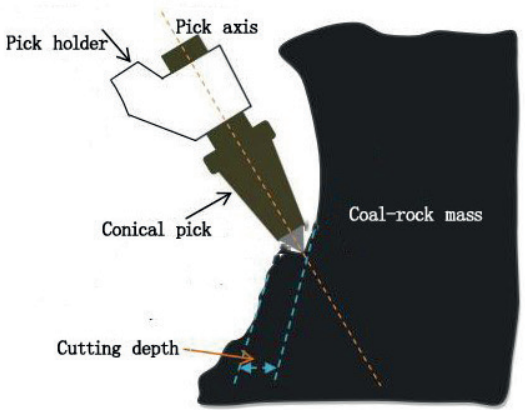

Fig. 1 Coal-rock cutting by a conical pick

For example, Xia [7] proposed a series of interaction numerical models for rock-breaking with the gage disc cutter by UDEC, and the Mohr-Coulomb constitutive model is adopted for marble. Ajibose [8] proposed indentation contact mechanics model for air hammer bit drilling. LSDYNA is a functional module of ANSYS, which has certain advantages in the aspect of rock cutting. In the simulation model, HJC dynamic constitutive model is adopted for rock by using LS-DYNA. Zhang [9] made an accuracy

Cite this article as: Qiao, S., Xia, J., Xia, Y., Liu, Z., Liu, J., Wang, A. "Establishment of Coal-rock Constitutive Models for Numerical Simulation of Coal-rock Cutting by Conical Picks", Periodica Polytechnica Civil Engineering, 63(2), pp. 456–464, 2019. https://doi.org/10.3311/PPci.13084

analysis to a dynamics simulation by using the ABAQUS software to study the process of continuously crushing hard rock under the rotary-impact load from a hydraulic drill, and the constitutive model of rock mass is Drucker-Prager model. In order to better simulate the process of coal-rock cutting, a new elastic-plastic-brittle constitutive model is established in this paper, the numerical realization of coal-rock constitutive can be utilized by ANSYS Parametric Design Language (APDL), so the corresponding calculation program is compiled by ANSYS. A comparison between the experiments and the simulation shows that the constitutive model can better be defined considering the coal-rock crushing process by a conical pick.

2 Coal-rock constitutive model

2.1 Coal-rock physical mechanics test

In order to obtain the constitutive model of coal-rock, the uniaxial compression test and Brazilian tensile test of coal-rock were carried out, and the macroscopic characteristics of coal-rock were obtained. As shown in Fig. 2, the coal-rock was loaded by the experimental system. And the tests were performed on core samples with length-to-diameter ratios of 2 and 1. Because of the consecutive loading, the final failure form of the samples can be observed clearly. The crushing process of coal-rock was photographed by digital camera.

According to the data and observations of uniaxial compression test, the crushing process of the coal-rock samples can be summarized as follows. Fig. 3(a) shows the state of the sample before loading. When the coal-rock sample is loaded at 0–15 kN, the axial size of the samples decreases with the increase of loading, but the deformation of coal-rock sample is not obvious. When the sample is loaded at 15 kN, the slip line appears on the surface of the sample, and the slip line has been through the whole sample when the sample is loaded at 15.8 kN. The slip state does not propagate obviously when the sample is loaded at 18 kN. When the sample is loaded at 18.5 kN, the crack appears on the sample and expands rapidly until the coal-rock failure, and the uniaxial pressure is about 19.5 KN. The slip failure stage is shown in Fig. 3(b) and the post- failure state is shown in Fig. 3(c).

Fig. 2 The experimental system

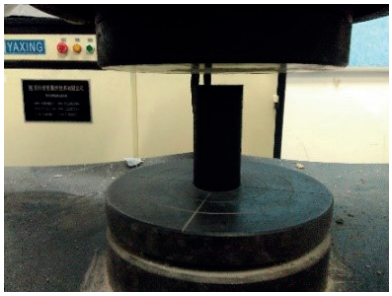

(a)

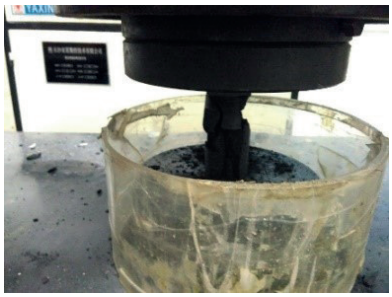

(b)

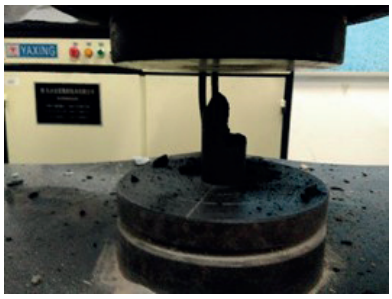

(c)

Fig. 3 The uniaxial compression test of coal-rock

The process of Brazilian tensile test can be summarized as follows. Fig. 4(a) shows the state of the sample before loading. When the coal-rock sample is loaded at 0–3.17 kN, the deformation of coal-rock sample is not obvious with the increase of loading. When the sample is loaded at 3.17 kN, the crack appears on the sample and expands rapidly until the coal-rock failure, and the uniaxial pressure is about 3.26 kN. The brittle failure stage is shown in Fig. 4(b) and the post-failure state is shown in Fig. 4(c).

2.2 Elastic-brittle-plastic model

Combined with the above analysis, the crushing process of the sample can be divided into four stages under uniaxial compression: elastic deformation stage, plastic stage, hardening stage and rheological stage.

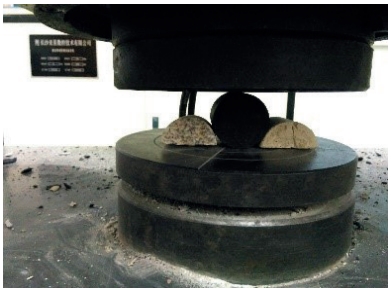

(a)

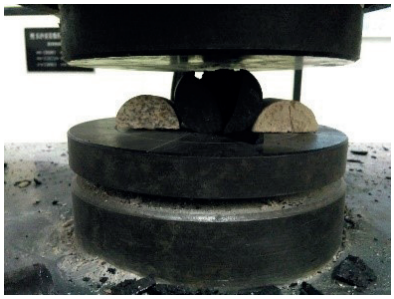

(b)

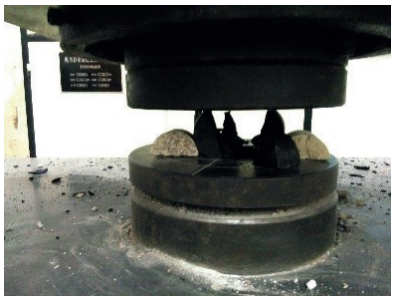

(c)

Fig. 4 The Brazilian tensile test of coal-rock

According to the relevant literature [10–14], the relatively mature constitutive model of coal-rock and it can be accepted by everyone is that the micro-elastic fracture of coal-rock is developed steadily in the first, which corresponds to the elastic deformation stage in macroscopic. And then, the unsteady fracture of coal-rock begins to develop, the macroscopic yield of coal- rock is shown, and the yield stress is about 2/3 of the peak strength. As shown in Fig. 5, this is the modified constitutive model of coal-rock, which is consistent with the previous experimental analysis. It is shown that the constitutive model can accurately describe the crushing process of coal-rock. *OA* is the elastic stage, the force is 0 kN ~ 15 kN. *AB* is the ductile strengthening stage after yielding, the force is 15 kN~ 15.8 kN. *BC* is the stress drop of the material failure, the force is 15.8 kN~ 18 kN. *CD* is the plastic rheological stage after shearing failure, that is, residual yield surface. *OE* is the elastic stage of element tension, the force is 0 kN~ 3.17 kN. *EF* is the stress drop of element tensile failure, the force is 3.17 kN~ 3.26 kN. *FG* is the stage after tensile failure. $\bar{\varepsilon}_f^p$ is a threshold for shear failure. S_t is a threshold for tensile failure. $\bar{\sigma}_Y^0$ is the uniaxial equivalent stress of initial yield. $\bar{\sigma}_Y^n$ is the uniaxial equivalent stress of shear failure. $\bar{\sigma}_r$ is the residual equivalent stress after material failure.

2.3 Development of constitutive model

Prediction of elastic stress values are obtained as follows:

$$\tilde{\sigma}_{ij}^k = \sigma_{ij}^{k-1} + D_{ijkl}^e \Delta\varepsilon_{ij}, \tag{1}$$

where $\tilde{\sigma}_{ij}^k$ is the predicted value of stress results calculated by k iterations. σ_{ij}^{k-1} is the value of stress results calculated by k–1 iterations. D_{ijkl}^e is fourth-order elastic stiffness tensor. $\Delta\varepsilon_{ij}$ is the strain increment.

The plastic-brittle damage constitutive equation is also discussed in this section. According to the failure criterion of literature [10], the compression damage variable and the tensile damage variable of equivalent plastic strain are established respectively.

$$\omega_c = \begin{cases} 0(\bar{\varepsilon}^{\mathrm{p}} < \bar{\varepsilon}_{\mathrm{f}}^{\mathrm{p}}) \\ \omega_c(\bar{\varepsilon}^{\mathrm{p}} \geq \bar{\varepsilon}_{\mathrm{f}}^{\mathrm{p}}) \end{cases}, \tag{2}$$

$$\omega_t = \begin{cases} 0(\left|\sigma_3^{el}\right| < S_t) \\ \omega_c(\left|\sigma_3^{el}\right| \geq S_t) \end{cases}, \tag{3}$$

where ω_e is compression damage value. ω_t is tensile damage value. $\bar{\varepsilon}^p$ is principal plastic strain in 3 directions. $\bar{\varepsilon}_f^p$ is equivalent plastic deformation of materials from yield state to failure state. σ_3^{el} is maximum tension stress. S_t is a threshold for tensile failure.

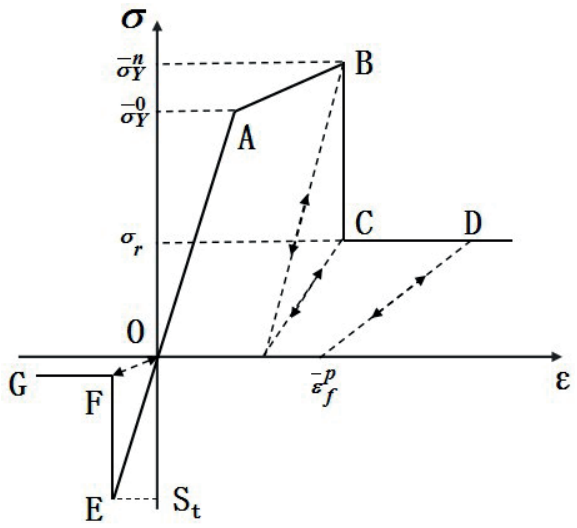

Fig. 5 The constitutive model of coal-rock

Therefore, the stress drop values of shear failure and tensile failure are obtained as follows:

$$\Delta\sigma_{ij}^{c} = D_{ijkl}^{e}\left(\varepsilon_{kl} - \varepsilon_{kl}^{p}\right)\omega_{c} . \tag{4}$$

$$\Delta\sigma_{ij}^{t} = D_{ijkl}^{e}\left(1-\omega_{t}\right)\omega_{c} . \tag{5}$$

where ε_{kl} is total strain. ε_{kl}^{p} is total plastic strain. D_{ijkl}^{e} is fourth-order elastic stiffness tensor.

According to the empirical formulas in literature [10], the inhomogeneity, anisotropy and multifissures of the coal -rock should be considered, so the statistical method should be used to describe them.

The probability density function of each parameter of the coal-rock may be written as a Weibull Distribution:

$$P\left(\sigma_{i}\right) = c_{i}m_{i}\left(\frac{\sigma_{i}}{\sigma_{i0}}\right)^{m_{i}-1}\exp\left[-\left(\frac{\sigma_{i}}{\sigma_{i0}}\right)\right]^{m_{i}}, \tag{6}$$

$$i = 1,2,\ldots,9;\ i \neq 3$$

where c_i is the normalized constant of the statistical function. mi is the morphological parameter of the statistical function, in this case, it is characterized as material inhomogeneity. i is the parameter number of the material. When i = 1, the probability density of the elastic modulus E of the material is described, and σ_i represents the elastic modulus E of the material. When i =7, the compressive strength limit σ_c of the material is described. All other material constants are expressed in this way, and σ_{i0} denotes the statistical average of the material parameters.

The macro file of material characteristic is compiled by the ANSYS Parametric Design Language (APDL). The distribution of material parameter value satisfies the Eq. (6). According to the characteristics of pseudo coal wall used in the experiment, a constitutive model of coal-rock is established. Each unit number is required to assign the material parameters one by one in the process of compiling the constitutive model, and a part of the constitutive model needs to be executed repeatedly. The macro file of the constitutive model is created by using command *create. In the LSDYNA analysis, the macro file is called by using command *USE, and the parameters are passed to the macro file, which ensures that the simulation results is closer to the experimental results. And the overall idea of the section can be expressed as Fig. 6.

Table 1 Numbers and symbols for nine material parameters of coal-rock

Serial number i	Representative symbol	Material property
1	E	Elastic modulus
2	μ	Poisson's ratio
3	t	Melting point
4	ρ	Density
5	σ_y/c	Thermal expansion coefficient
6	$\tilde{H}$	Hardening coefficient
7	σ_b	Compressive strength
8	S_t	Tensile strength
9	ϕ	Internal friction angle

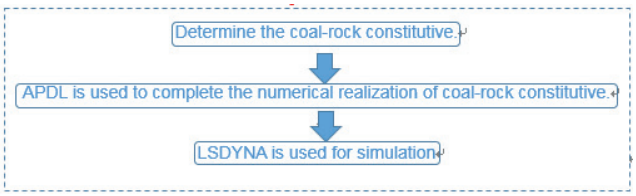

Fig. 6 The overall idea of simulation

Table 2 Material parameters of coal-rock

Material property	Material parameters
Elastic modulus/GPa	3.5
Poisson's ratio	0.3
Melting point/℃	1440
Density (kg/m^3)	1851
Thermal expansion coefficient	1.186
Hardening coefficient	1
Compressive strength /MPa	19.5
Tensile strength/MPa	1.3
Internal friction angle/(°)	52

3 Application of coal - rock constitutive model

3.1 Numerical modelling

At present, a large number of simulation about rock-cutting have been done at home and abroad [1, 3, 15–22]. For verifying the accuracy of the elastic-brittle-plastic constitutive model, numerical simulation and experimental study were carried out. The materials properties of coal wall are the same as those of coal-rock in uniaxial test. The mechanical index of coal-rock is given in Table 2. The simulation model of coal-rock cutting was established (see Fig. 7), in which the conical pick interacts with the coal-rock. And the cutting depth d was set to 9 mm.

3.2 Numerical simulation

As shown in Fig. 8, the interface between the conical pick and coal-rock produces extrusion deformation. At the yield strength limit of the coal-rock, the moving pick induces radial and tension cracks. The interface between the pick and coal-rock is gradually damaged, and the damage area

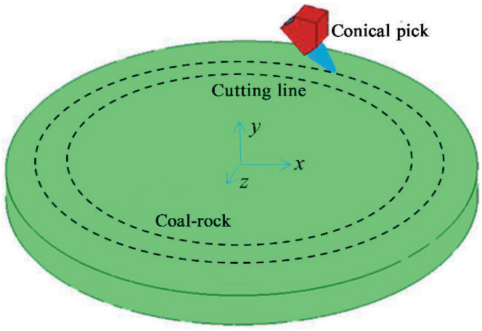

Fig. 7 Coal-rock cutting simulation model

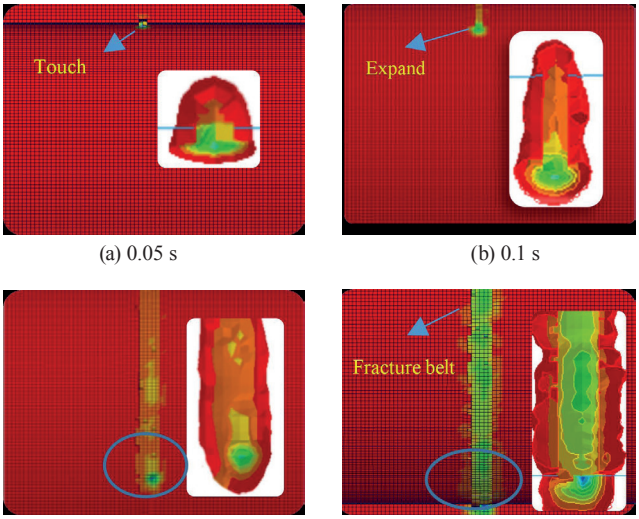

(a) 0.05 s (b) 0.1 s

(c) 0.15 s (d) 0.2 s

Fig. 8 Fragmentation process of coal-rock

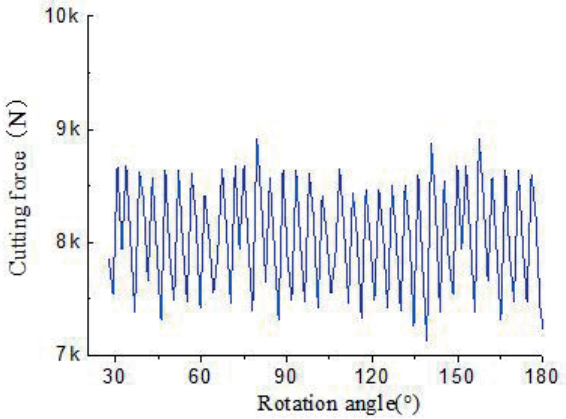

Fig. 9 Cutting force at $d = 9$ mm

of the coal-rock gradually increases with the rotation of the cutting head. A partial fracture belt appears on the interface between the conical pick and coal-rock.

The leap-forward breakage is an obvious characteristic in the process of coal-rock cutting. The cutting force increases with the increase of cutting depth when the conical pick begins to intrude into coal-rock. When a certain critical value is reached, a sudden leap of cutting force occurs. The coal-rock collapses at the same time, and the cutting force decreases instantaneously. As the conical pick moves forward to the new surface formed by the contact fracture, a new cycle begins again. Fig. 9 shows the curve of cutting force at $d = 9$ mm. During the initial contact between the conical pick and coal-rock, a large number of small pieces of debris are formed, and each peak point in the curve corresponds to a leap-forward breakage.

Also, coal-rock cutting simultaneously by two conical picks was studied. The cutting depth d was set to 9, 15, 20, 26, 33 mm, the cutting space s is set to 35, 50, 65, 70, 80 mm.

The specific energy consumption is calculated by Eq. (7).

$$SE = \frac{W}{V} = \frac{\bar{T}tn}{9550 \times 3600V}, \tag{7}$$

where SE is the specific energy (kWh/m^3), V is the cutting volume (m^3), n is the rotation rate of the cutting head (r/min) and t is the cutting time (s).

As shown in Fig. 10, for a given cutting space, increasing the cutting depth decreases the specific energy consumption up to a certain depth. Beyond this minimum, the specific energy consumption increases with cutting depth. The trend is gentle because the fragmentation volume of the coal-rock is very small at small cutting depths, which increases the specific energy consumption. As the cutting depth increases, the fragmentation volume of the coal-rock increases and the specific energy consumption is optimised at a certain cutting depth.

For a given cutting depth, the specific energy consumption also decreases with increasing cutting space, then increases. When the coal-rock is cut in relieved cutting mode (see Fig. 11a) and the cutting space is too small, considerable overcutting or grinding occurs, which increases the specific energy consumption. When the coal-rock is cut

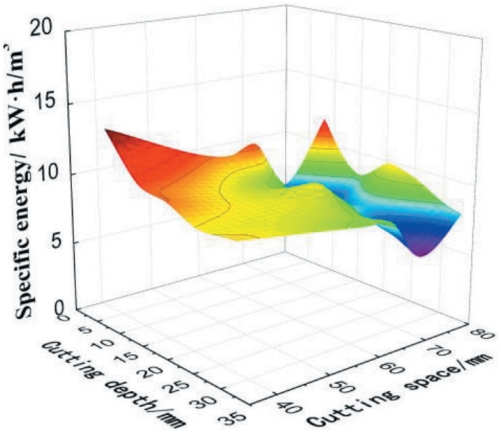

Fig. 10 Relation between specific energy and cutting depth

in unrelieved cutting mode (see Fig. 11b), chunks of debris are not formed, and the energy consumption is higher than in relieved cutting mode. As shown in Fig. 9, the specific energy consumption is minimised at a particular cutting space and cutting depth. The specific energy consumption of the cutting head cannot be minimised by a single variable; instead, the optimisation requires a comprehensive investigation of the relation between the two variables. Fig. 12 is a scatter plot of the specific energy consumption calculated by Eq. (6) versus the *s*/*d* index. The specific energy consumption initially decreases and then increases with increasing s/d. The s/d of the lignite sample is optimised at around 2.7–3.3.

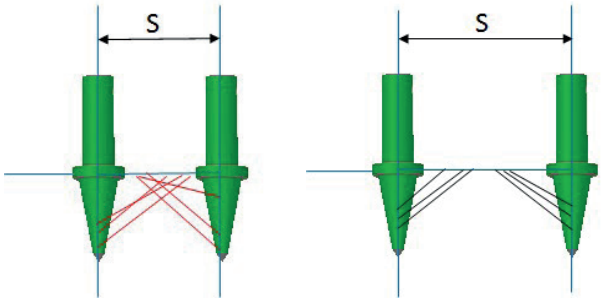

(a) relieved cutting mode (b) unrelieved cutting mode

Fig. 11 Two modes of cutting the coal-rock

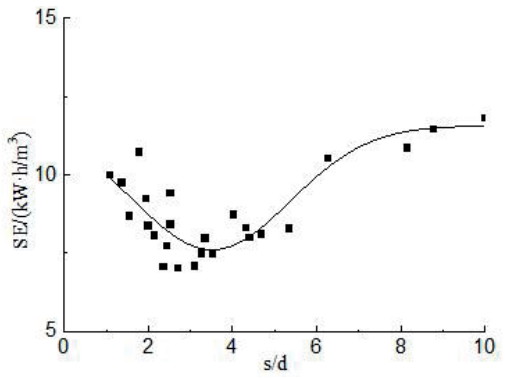

Fig. 12 Relation between specific energy and *s*/*d*

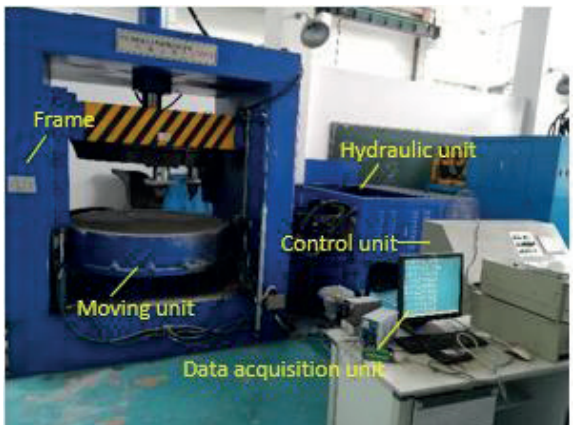

Fig. 13 Coal-Rock Cutting Machine (CCM) in CSU

4 Experimental study

A large number of rock cutting experiments have been done at home and abroad [2, 23–27].The experiments were conducted on the Coal-rock Cutting Machine (CCM) in Central South University. As shown in Fig. 13, the main components of the CCM are the frame, the moving unit, the hydraulic unit, the control unit and the data acquisition unit. Driven by the specimen bed of the CCM, the sample box rotates and the conical pick are cut into the coal-rock. The cutting force was recorded by data acquisition unit. The cutting material in this experiment was the same as in the uniaxial compression test. Two experiments were conducted as follows, and the cutting space was 70 mm. The experimental cutting depth was 9 mm.

1. The coal-rock was cut twice successively by a conical pick.
2. The coal-rock was cut simultaneously by two conical picks.

4.1 Two cuts successively by a conical pick

The two cuts were carried out successively in the cutting experiments (see Fig. 14). During the first cut, with the continuous rolling of the conical pick, the conical pick is constantly pressed into the coal-rock. The crushing zone is extruded and cracks develop on both sides of the pick-tips. As the cracks expand, the coal-rock breaks down into small pieces. As shown in Fig. 15, the cutting force increases gradually in the first when the pick-tip keeps grinding the coal-rock surface. Afterwards, the cutting force fluctuates in the range between 7 kN and 9 kN when the coal-rock begin to break. The averaged peak values of the cutting forces and the specific energy (*SE*) of the first cut are measured as 8.5 kN, 20.1 MJ/m^3 respectively. As shown in Fig. 14, the size of small piece at second cut is relatively larger than the first cut. This may be because that it forms some crack at first cut or at second cut, and the crack is coalescent at second cut.

Fig. 15 shows that the cutting force at the second cut is obviously lower than the first cut. This may be because of that the removal of the chips produced in the first cut resulted in many voids in the coal-rock surface, and the second cut is easier to break coal-rock. It can be stated that the coal-rock cutting force and specific energy of the first cut may be a little higher than real, but acceptable for verification with limitations in accuracy. As a result, the first cut were all used to verify the numerical models.

Error analysis of cutting force and specific energy are shown in Fig. 16. A comparison between the two experiments and the simulation shows they were in reasonable

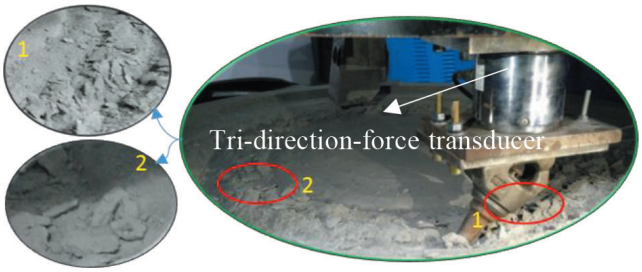

Fig. 14 Coal-rock fragmentations at $d = 9$

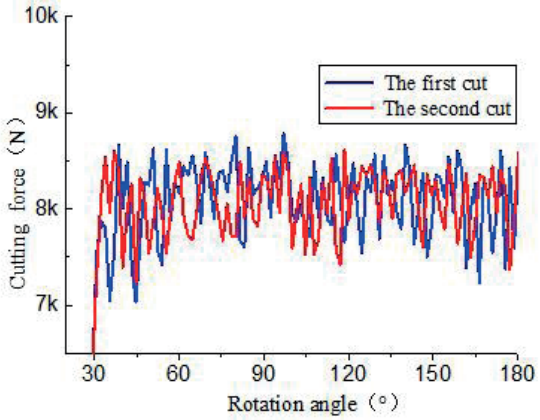

Fig. 15 Components of the cutting force at $d = 9$mm

agreement. Only the first cut is used to verify the numerical models. It can be seen that the cutting forces in the simulation are similar to the first cut with a relative error of about 13.5 %. The total error is the smallest since the relative errors of the cutting force and specific energy are all small. The total error between the simulation and experimental values (8.5 %) is within a reasonable range, verifying the correctness of the simulation model. It indicates that the coal-rock constitutive model is close to real whereby the simulations may be more or less accurate.

4.2 Coal-rock cutting simultaneously by two conical picks

Also, the experiments of coal-rock cutting by two conical picks were studied (see Fig. 17). Because of the limitations of the cutting experiment, the experimental cutting depth (VDep) was set to 6 mm, 9 mm, 12 mm, or 15 mm.

The experimental and simulation results are compared in Fig. 18, which plots the measured and simulated cutting forces of the conical picks at four cutting depths. As the cutting depth VDep increases from 6 to 15 mm, the actual cutting force increases similarly to the simulated data. The slight differences between the measured and simulated cutting forces at VDep = 12 and 15 mm can be explained by uncontrollable factors that increase with increasing cutting depth. Whereas the simulation was carried out under ideal

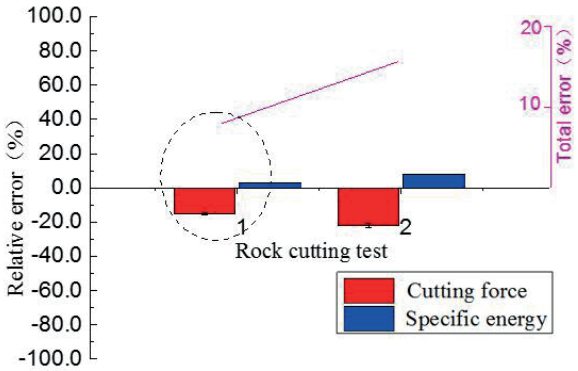

Fig. 16 Error analysis of cutting force and specific energy to the two experiments

Fig. 17 Coal-rock cutting simultaneously by two conical picks

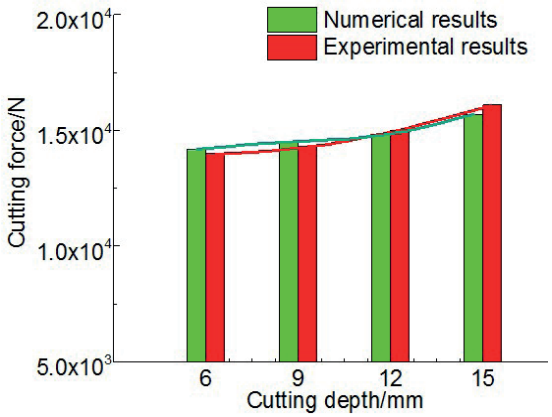

Fig. 18 Relation between cutting force and cutting depth

conditions, the actual testing system is subjected to many external disturbances, such as heterogeneity of the coal-rock. The maximum deviation between the simulation and experimental values (9.8 %) is within a reasonable range.

From the view of the fracture form of coal-rock and the performance of coal-rock cutting, the simulation and experiment can agree well with each other. The rationality of the constitutive model is proved subjectively.

5 Conclusions

In this paper, the coal-rock cutting models was simulated and the results were compared with coal-rock cutting experiment on a Coal-rock Cutting Machine. The main conclusions are as follows:

3. Combined with previous experience formula, the numerical model of elastic-brittle-plastic constitutive model of coal-rock is established through uniaxial compression test of coal- rock.
4. The model can correctly reflect the damage of coal-rock. A comparison between the two experiments and the simulation shows they were in reasonable agreement. The total error between the simulation and experimental values is within a reasonable range.
5. The elastic-brittle-plastic constitutive model of coal-rock in this paper can be used to pre-evaluate the characteristics of coal- rock cutting by conical picks, and the simulation results can provide reasonable suggestions for pick layout of cutting head.

Acknowledgment

This research was supported by the Strategic Emerging Industry Technology Research Program of Hunan (2015GK1009), and the Fundamental Research Funds for the Central Universities of Central South University (2017zzts094).

References

[1] Yasar, S., Yilmaz, A. O. "A Novel Mobile Testing Equipment for Rock Cuttability Assessment: Vertical Rock Cutting Rig (VRCR)", Rock Mechanics and Rock Engineering, 50(4), pp. 857–869, 2017. https://doi.org/10.1007/s00603-016-1149-z

[2] Kahraman, E., Kahraman, S. "The performance prediction of roadheaders from easy testing methods", Bulletin of Engineering Geology and the Environment, 75(4), pp. 1585–1596, 2016. https://doi.org/10.1007/s10064-015-0801-2

[3] Jang, J.-S., Yoo, W.-S., Kang, H., Cho, J.-W., Jeong, M.-S., Lee, S.-K., Cho, Y.-J., Lee, J.-W. "Cutting head attachment design for improving the performance by using multibody dynamic analysis", International Journal of Precision Engineering and Manufacturing, 17(3), pp. 371–377, 2016. https://doi.org/10.1007/s12541-016-0046-4

[4] Baldwin, J. "Innovation in roofbolted development roadways the Voest Alpine ABM 20 continuous miner bolter", CIM Bulletin, 89(1000), pp. 40–45, 1996.

[5] Leeming, J., Flook, S., Altounyan, P. "Bolter miners for longwall development", Gluckauf: Die Fachzeitschrift fur Rohstoff, Bergbau und Energie, 137(11), pp. 633–637, 2001.

[6] Vierhaus, R. "Development of a high-performance drivage by "Bolter-Miner" technology", Gluckauf: Die Fachzeitschrift fur Rohstoff, Bergbau und Energie, 138(9), pp. 425–429, 2002.

[7] Xia, Y.-M., Wu, Y., Guo, J.-C., Tian, Y.-C., Lin, L.-K., Bian, Z.-K. "Numerical simulation of rock-breaking mechanism by gage disc cutter of TBM", Journal of China Coal Society, 39, pp. 172–178, 2014. https://doi.org/10.13225/j.cnki.jccs.2013.0177

[8] Ajibose, O. K., Wiercigroch, M., Akisanya, A. R. "Experimental studies of the resultant contact forces in drillbit-rock interaction", International Journal of Mechanical Sciences, 91, pp. 3–11, 2015. https://doi.org/10.1016/j.ijmecsci.2014.10.007

[9] Zhang, Q., Suo, J.-W., Wang, H.-J., Sun, G.-Q., Sun, H.-W. "Numerical simulation analysis on the drill bit rock breaking process based on ABAQUS", Journal of Vibration and Shock, 37, pp. 136–141, 2018. https://doi.org/10.13465/j.cnki.jvs.2018.01.021

[10] Indraratna, B., Nimbalkar, S., Coop, M., Sloan, S. W. "A constitutive model for coal-fouled ballast capturing the effects of particle degradation", Computers and Geotechnics, 61, pp. 96–107, 2014. https://doi.org/10.1016/j.compgeo.2014.05.003

[11] Liu, H., Cheng, Y., Zhao, C., Wang, H., Chen, H. "Constitutive Model For Elasto-Brittle-Plastic Damage Of Coal Rock Mass Due To Mining And Its Application", Chinese Journal of Rock Mechanics and Engineering, 29, pp. 358–365, 2010.

[12] Yu, W. J., Du, S. H., Wang, W. J. "Prediction of instability and mechanism of multi-factor comprehensive action on mine goaf", International Journal of Engineering Research in Africa, 13, pp. 39−48, 2014. https://doi.org/10.4028/www.scientific.net/JERA.13.39

[13] Sarfarazi, V., Haeri, H., Marji, M. F., Zhu, Z. "Fracture Mechanism of Brazilian Discs with Multiple Parallel Notches Using PFC2D", Periodica Polytechnica Civil Engineering, 61(4), pp. 653−663, 2017. https://doi.org/10.3311/PPci.10310

[14] Xu, T., Ranjith, P. G., Au, A. S. K. Wasantha, P. L. P., Yang, T. H., Tang, C. A., Liu, H. L., Chen, C. F., "Numerical and experimental investigation of hydraulic fracturing in Kaolin clay", Journal of Petroleum Science and Engineering, 134, pp. 223–236, 2015. https://doi.org/10.1016/j.petrol.2015.08.003

[15] Heydarshahy, S. A., Karekal, S. "Investigation of PDC cutter interface geometry using 3D FEM modelling", International Journal of Engineering Research in Africa, 29, pp. 45–53, 2017. https://doi.org/10.4028/www.scientific.net/JERA.29.45

[16] Qiao, S., Xia, Y., Liu, Z., Liu, J., Ning, B., Wang, A. "Finite element analysis of load characteristic of shield bolter miner cutting head under complex coal seam condition", Mining Science, 24, pp. 85–97, 2017. https://doi.org/10.5277/msc172405

[17] Esterhuizen, G. S., Tulu, I. B. "Analysis of alternatives for using cable bolts as primary support at two low-seam coal mines", International Journal of Mining Science and Technology, 26(1), pp. 23–30, 2016. https://doi.org/10.1016/j.ijmst.2015.11.005

[18] Mężyk, A., Klein, W., Fice, M., Pawlak, M., Basiura, K. "Mechatronic model of continuous miner cutting drum driveline", Mechatronics, 37, pp. 12–20, 2015.
https://doi.org/10.1016/j.mechatronics.2015.11.004

[19] Shao, W., Li, X., Sun, Y., Huang, H. "Parametric study of rock cutting with SMART*CUT picks", Tunnelling and Underground Space Technology, 61, pp. 134–144, 2017.
https://doi.org/10.1016/j.tust.2016.09.012

[20] Eyyuboglu, E. M., Bolukbasi, N. "Effects of circumferential pick spacing on boom type roadheader cutting head performance", Tunnelling and Underground Space Technology, 20(5), pp. 418–425, 2005.
https://doi.org/10.1016/j.tust.2005.02.002

[21] Kang, H., Cho, J.-W., Park, J.-Y., Jang, J.-S., Kim, J.-H., Kim, K.-W., Rostami, J., Lee, J.-W. "A new linear cutting machine for assessing the rock-cutting performance of a pick cutter", International Journal of Rock Mechanics and Mining Sciences, 88, pp. 129–136, 2016.
https://doi.org/10.1016/j.ijrmms.2016.07.021

[22] Xia, Y., Shi, Y., Lin, L., Zhang, Y., Tan, Q., Yang, Y. "Experimental Evaluation of Fragments from TBM Disc Cutting under Different Load Cases", Periodica Polytechnica Civil Engineering, 62(3), pp. 746−756, 2018.
https://doi.org/10.3311/PPci.11961

[23] Yilmaz, N. G., Tumac, D., Goktan, R. M. "Rock cuttability assessment using the concept of hybrid dynamic hardness (HDH)", Bulletin of Engineering Geology and the Environment, 74(4), pp. 1363–1374, 2015.
https://doi.org/10.1007/s10064-014-0692-7

[24] Hartlieb, P., Grafe, B., Shepel, T., Malovyk, A., Akbari, B. "Experimental study on artificially induced crack patterns and their consequences on mechanical excavation processes", International Journal of Rock Mechanics and Mining Sciences, 100, pp.160–169, 2017.
https://doi.org/10.1016/j.ijrmms.2017.10.024

[25] Yasar, S., Yilmaz, A. O. "Rock cutting tests with a simple-shaped chisel pick to provide some useful data", Rock Mechanics and Rock Engineering. 50(12), pp. 3261–3269, 2017.
https://doi.org/10.1007/s00603-017-1303-2

[26] Copur, H., Bilgin, N., Balci, C., Tumac, D., Avunduk, E. "Effects of different cutting patterns and experimental conditions on the performance of a conical drag tool", Rock Mechanics and Rock Engineering, 50(6), pp. 1585–1609, 2017.
https://doi.org/10.1007/s00603-017-1172-8

[27] Kim, E., Hirro, K., Oliveira, D., Kim, A. "Effects of the skew angle of conical bits on bit temperature, bit wear, and rock cutting performance", International Journal of Rock Mechanics and Mining Sciences, 100, pp. 263–268, 2017.
https://doi.org/10.1016/j.ijrmms.2017.11.006